

INNOVATIVE OPTICAL TACTILE SENSOR FOR ROBOTIC SYSTEM BY GOLD NANOCOMPOSITE MATERIAL

A. Massaro and F. Spano

Center of Bio-Molecular Nanotechnologies
Italian Institute of Technology IIT, Arnesano 73100, Italy

P. Cazzato

National Nanotechnology Laboratory
Institute of Nanoscience of CNR, Lecce 73100, Italy

R. Cingolani

Italian Institute of Technology IIT
Via Morego 30, Genova 16163, Italy

A. Athanassiou [†]

Center of Bio-Molecular Nanotechnologies
Italian Institute of Technology IIT, Arnesano 73100, Italy

Abstract—In this work we propose a new class of optical pressure sensors suitable for robot tactile sensing. The sensors are based on a tapered optical fiber, where optical signals travel, embedded into a PDMS-gold nanocomposite material. By applying different pressure forces onto the PDMS-based nanocomposite we measure in real time the change of the optical transmittivity due to the coupling between the gold nanocomposite material and the tapered fiber region. The intensity reduction of the transmitted light intensity is correlated with the pressure force magnitude.

Received 25 November 2010, Accepted 1 January 2011, Scheduled 13 January 2011

Corresponding author: Alessandro Massaro (alessandro.massaro@iit.it).

[†] Also with National Nanotechnology Laboratory, Institute of Nanoscience of CNR, Lecce 73100, Italy.

1. INTRODUCTION

Sensory information of human skin for feeling materials and determining their physical properties is provided by sensors introduced under skin. Presently, many researchers are attempting to apply the five senses to intelligent robot systems. In particular, many kinds of tactile sensors combining small force sensors have been introduced into intelligent robots. These tactile sensors, which are capable of detecting contact force, vibration, texture, and temperature, can be recognized as the next generation of information collection system. Future applications of engineered tactile sensors include robotics in medicine for minimally invasive microsurgeries, military uses for dangerous and delicate tasks, and automation in industries. Some tactile sensors and small force sensors using microelectromechanical systems (MEMS) technology have been introduced. MEMS tactile sensing work has been focused mainly on silicon-based sensors that use piezoresistive [1–3] or capacitive sensing [4–6]. These sensors have been realized with bulk and surface micromachining methods. Polymer-based devices that use piezoelectric polymer films [7–9] such as polyvinylidene fluoride (PVDF) for sensing have also been demonstrated. Although these sensors offer good spatial resolution due to the use of MEMS techniques, they still have problems in applications to practical systems. In particular, devices that incorporate brittle sensing elements such as silicon based diaphragms or piezoresistors, are not reliable for robotic manipulation. Previous efforts have been hindered by rigid substrates, fragile sensing elements, and complex wiring. These drawbacks can be compensated by utilizing flexible optical fiber sensors and transducers. In addition, optical fiber sensors are immune to electromagnetic fields, can be easily multiplexed and integrated with small LED sources, thus providing a good alternative for the implementation of robotic tactile sensors [10]. A first prototype was based on a non-integrated cap of PDMS-Au material just placed on tapered fiber [11]. For this first prototype, we have observed a low sensitivity in the order of about 20 grams. In this paper we present a newly designed optical fiber force sensor prototype based on electromagnetic (EM) coupling effect of totally embedded tapered fiber in gold nanocomposite material (GNM).

2. THEORY: BASIC PRINCIPLE

The sensors illustrated in Figs. 1(a)–(d) are the optimized version obtained after previous preliminary studies [11] where the key parameter was the PDMS-gold controlled thickness: in the optimized

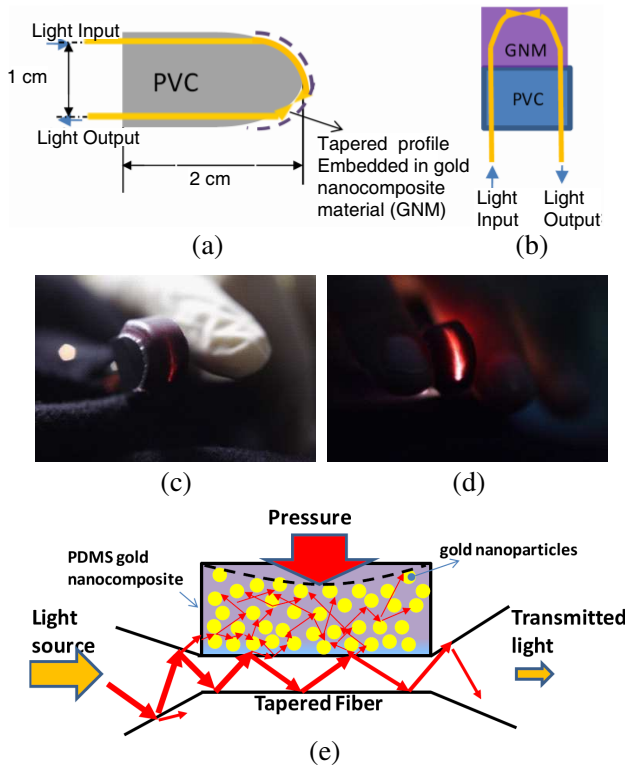


Figure 1. (a) and (b) Layouts of optical pressure sensor implemented in robotic system: a tapered optical fiber is bended on a PVC support and embedded in a PDMS-Au material (GNM). (c) and (d) Photos of the first prototype (the PDMS-Au cladding is 5 mm thick). (e) Light coupling and scattering process inside the GNM.

version of the sensor the whole diameter of the tapered fiber is embedded in the GNM thus increasing the sensor sensitivity. An optical ray coming from a broad lamp source is dispersed inside the gold nanocomposite material when the sensor is pressed on a surface: this effect is due to the electromagnetic coupling of the tapered fiber with the PDMS-Au material which provides a reduction of the transmitted signal. The gold nanoparticles formed in the PDMS material are expected to increase the effective refractive index of the PDMS and support the electromagnetic coupling with the tapered region of the fiber, since the transmitted light tends to preferentially propagate into the high refractive index regions. The pressure applied on the GNM introduces a displacement of the nanoparticles along its interface with

the tapered fiber increasing the light scattering [11] (see Fig. 1(e)): the nanoparticles thus increase the coupling of light with the GNM, reducing the transmitted light intensity of the optical fiber. Regarding the modifications of the optical properties of the GNM, the effect of the nanoparticle displacements due to the applied pressure is to change the effective refractive index of GNM as a function of gold concentration. In particular the gradual variation of the GNM effective refractive index is higher near the contact interface of the tapered fiber, and, lower towards the pressure contact surface. We can model the gradual variation of the GNM effective refractive index as illustrated in Figs. 2(a)–(c), where the region with higher refractive index is near the contact interface of the tapered fiber, and, the region with lower effective refractive index is towards the pressure contact surface. This variation of the effective refractive index can be approximately estimated assuming spherical gold nanoparticles in PDMS material. In this case the effective dielectric function ε_{eff} for spherical gold particles having dielectric function ε_m which varies with the optical working wavelengths [11], embedded in a medium ε_s is defined by [12, 13] as:

$$\varepsilon_{eff} = \varepsilon_s \frac{\varepsilon_m(1 + 2\phi) + 2\varepsilon_s(1 - \phi)}{\varepsilon_m(1 - \phi) + \varepsilon_s(2 + \phi)} \quad (1)$$

where ϕ indicates the gold concentration.

The modes of the tapered fiber will exchange the power with PDMS-Au cladding by defining the coupling coefficient as follow [14]

$$C_{\psi_{nm}, E^r}(z) = \omega \int_{-\infty}^{\infty} \int_{-\infty}^{\infty} \Delta\varepsilon_{eff}(z) \psi_{nm} E^r dx dy \quad (2)$$

where ψ_{nm} are the fiber modes, E^r is the electric evanescent field radiated by the tapered profile, and, $\Delta\varepsilon_{eff}$ indicates the variation of the effective permittivity of the cladding due to different applied forces. According with (2), we observe that the coupling can be increased by bending the tapered fiber as shown in Figs. 1(a) and (b).

The displacement of the gold nanoparticles in PDMS due to a uniformly applied force are schematically indicated by the bidimensional (2D) mechanical finite element method (FEM) simulation of Fig. 2(a): the particles which are on the top of the GNM microcell region tend to accumulate near the contact interface by increasing the effective dielectric function of ε_{eff} due to the increment of ϕ as schematized in Fig. 2(b). The exact distribution of the function ε_{eff} during the applied force is very difficult to model. In order to explain the basic principles by an approximated model, we assume high gold concentration for the region with higher effective

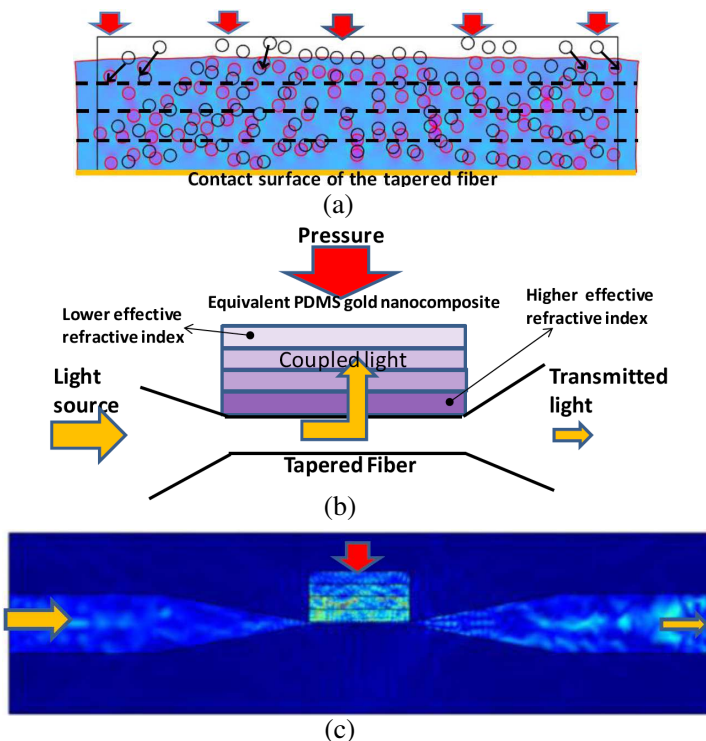


Figure 2. (a) 2D mechanical FEM modeling of a GNM microcell: gold nanoparticle displacements due to an applied force. The simulated particles have a diameter of 120 nm. (b) Equivalent nanocomposite material as gradual variation of the effective refractive index. (c) 2D electromagnetic FEM modeling: simplified modeling obtained by reducing by a factor of 2 the value of the effective permittivity (corresponding to a theoretical reduction of gold concentration). The light coupling effect is more effective closed to the tapered fiber interface.

permittivity in contact with the tapered region, and a reduction of ϵ_{eff} of different extent. The 2D electromagnetic (EM) FEM simulation of Fig. 2(c) shows that the EM energy is confined where the effective permittivity is higher (pressure effect) by reducing the transmitted light intensity at the output of the fiber. The parameters used in the FEM simulation are: λ_0 (working wavelength) = 1.3 μm , ϵ_{fiber} (relative dielectric permittivity of the core of the tapered fiber) = 3.17, ϵ_s (relative dielectric permittivity of PDMS) = 2.25, $\epsilon_{eff} = 10$ (real part of the relative dielectric permittivity of the first layer of GNM of Fig. 2(b)

with $\phi = 0.5$), ρ_{gold} (density of gold) = 19300 kg/m^3 , ρ_{PDMS} (density of PDMS) = 970 kg/m^3 , E_{gold} (Young's modulus of gold) = $70 \cdot 10^9 \text{ Pa}$, E_{PDMS} (Young's modulus of PDMS) = $500 \cdot 10^3 \text{ Pa}$, ν_{gold} (Poisson's ratio of gold) = 0.44 , ν_{PDMS} (Poisson's ratio of PDMS) = 0.5 .

We have used as FEM tool a properly designed tool, evolution of a tool oriented on electromagnetic problems [15].

3. OPTICAL CHARACTERIZATION, TECHNOLOGICAL ASPECTS AND DISCUSSIONS

The two proposed prototype sensor layouts are illustrated in Fig. 1(a): a tapered multimode Silica fiber couples the EM field coming from a broad band lamp source with the flexible polymer-gold nanocomposite material (PDMS-Au). The sensors are designed in order to improve a high sensitivity for low applied pressure forces: the design considers the double radiation effect due to the bending loss effect and to the radiation of the tapered profile [16].

By this double effect we will obtain high coupling coefficients (2) due to the high intensive evanescent E^r fields, and, consecutively, high sensor sensitivities. Moreover, we consider a multimode optical fiber because it is characterized by a big core diameter if compared to the diameters of the single mode fibers: in this case more contact interface

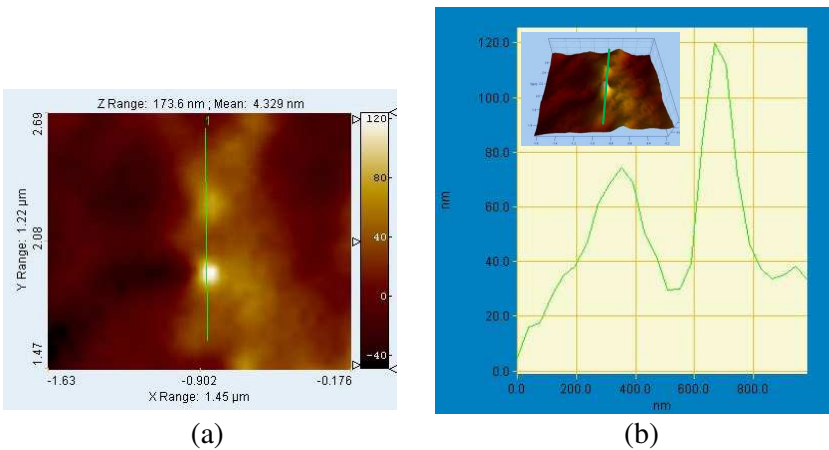


Figure 3. Nanoscale dimension of the gold particles: Atomic Force Microscopy (AFM) images made on cross section of the PDMS gold nanocomposite material. (a) Error signal and (b) error signal plot along a line. Inset: 3D plot of the error signal.

will increase the coupling efficiency. Polydimethylsiloxane (PDMS) polymer film was chosen for the proposed sensor due to its ability to generate gold nanoparticles starting from gold precursors [17, 18]. Moreover PDMS presents good elastomeric properties which allow to obtain a real time pressure sensor response of the order of 0.6 seconds (DMA mechanical measurements). The Atomic Force Microscopy (AFM) images of the cross section of the GNM shown in Fig. 3 provide information on the dimensions of the nanofillers inside the PDMS nanocomposite material. Previous studies demonstrate that the use of the PDMS polymer is able to generate gold nanoparticles by reducing the gold precursor [12, 13]. In our study we establish a very high gold concentration which anyway preserves the elastomeric properties of the GNM for the real time pressure detection. In the specific case, we use a chlorauric acid salt as gold precursor in water solution ($M_w(\text{HAuCl}_4) = 339.785 \text{ g/mol}$; $[\text{HAuCl}_4] = 0.01 \text{ M}$) with a concentration of about 10% in weight. Concerning the prototype of Fig. 1(a), the tapered fiber is fabricated by a coated silica / core silica multimode optical fiber (FG-365-LER Thorlabs fiber with a core of $365 \mu\text{m}$) by a homemade controlled system in order to improve a 0.8 cm of the total tapered profile with about 3 mm of central core

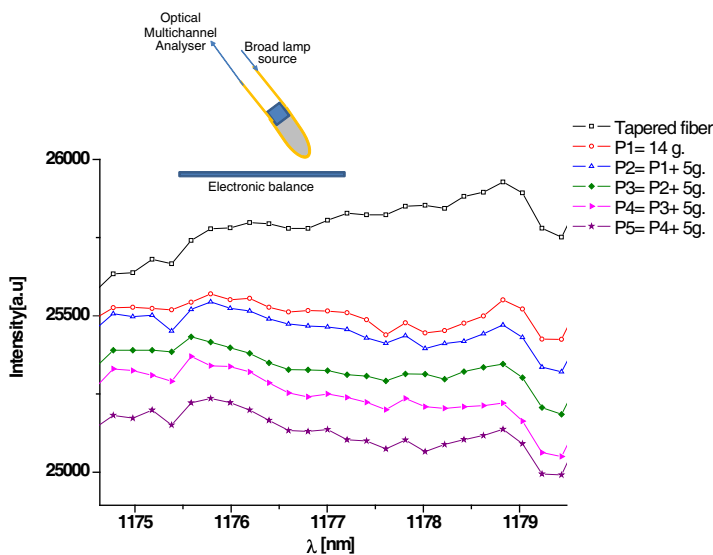


Figure 4. Optical transmittivity in function of applying different equivalent weights. Inset: schematic diagram of the experimental setup.

region without cladding. According with the experimental results of Fig. 4 we found a sensitivity of few grams in an optical wavelength range when the sensor is pressed on an electronic balance. The pressure on the balance will define the equivalent weight P which is indicated on the balance's screen. We observe that the reduction of the intensity after the application of weights is observed in the whole OMA range (800 nm–1400 nm), and, Fig. 3 reports only a zoomed part of the whole range in order to distinguish better the measurements.

During the experimentation of the prototype of Fig. 1(a) we use a controlled mechanical stage able to avoid the misalignment of the whole system (fiber/PDMS-Au). The reported measurements are the average value of five series of measurements. The measurements are repeated in different times by providing repeatable results with very low errors. The repeatability of the measurements is possible also due to the elastomeric properties of the GNM: in fact, the elastomeric pressure response remains stable during time. As also proved by Fig. 5 this transmittivity reduction of the optical intensity is found at different working wavelengths according also with the modal characteristics of the multimodal fiber used in the experimental setup.

As shown in Fig. 5, the use of the multimode fiber allows to analyze the different coupling behavior of the fiber modes ψ_{nm} in the whole range of the optical multichannel analyzer (OMA) connected to the output of the tapered fiber in order to read with a very high accuracy the transmitted light intensity. In this way it is possible to increase

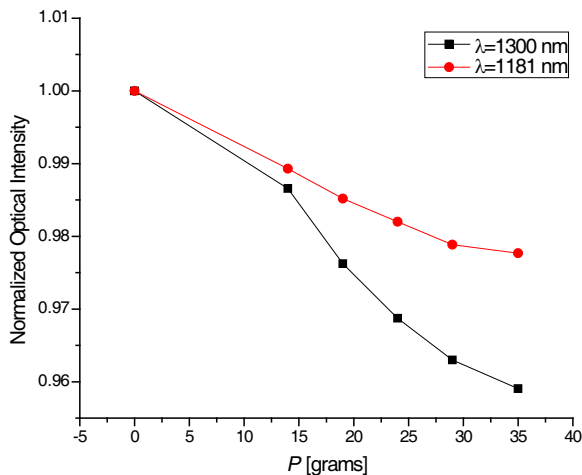


Figure 5. Sensitivity responses: optical transmittivity versus the applied weight P at different working wavelengths.

the efficiency by fixing the working wavelength exhibiting the best sensitivity. A laser diode operating at this frequency will represent the proper source for the tactile sensor.

The measured prototype of Fig. 1(a) exhibits a very high sensitivity but, being the tapered fiber positioned directly on the rigid PVC support, it is not suitable for high pressure forces. For this purpose we have designed the sensor layout of Fig. 1(b). As illustrated in Fig. 6(a), the cylindrical PVC support has different holes which will be filled by the GNM in order to improve a major mechanical stability and a good adhesion with the PVC support. The optical fiber is passed through two external holes (see Fig. 6(b)), and a glue is added in these external holes in order to fix the fiber. The PVC support allows to fix the optimum radius of curvature of the fiber for the tapered process (heating controlled system).

4. ELECTRIC CHARACTERIZATION AND SENSOR SENSITIVITY

The implementation of the proposed sensor in a robotic system requires the conversion of the optical signal into an electrical one: a photodiode allows this opto/electrical conversion and, consecutively, the signal can be processed by an intelligent electronic system able to perform detection of shapes or surface roughness. The sensor of Fig. 1(b) is fixed on an electronic balance (see Fig. 7) which measures the equivalent applied weight. The pressure forces is performed by a

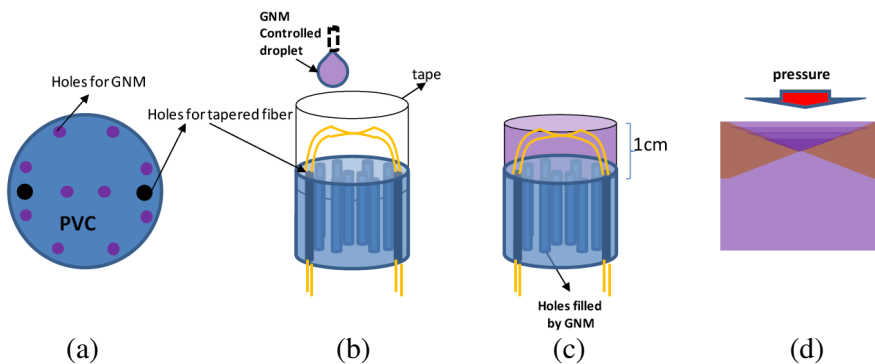


Figure 6. (a) Top view of the PVC support. (b) Controlled deposition of liquid GNM droplets. (c) Sensor layout after the GNM deposition process. (d) Schematic sketch of the pressure effect: equivalent GNM as gradual variation of the effective refractive index.

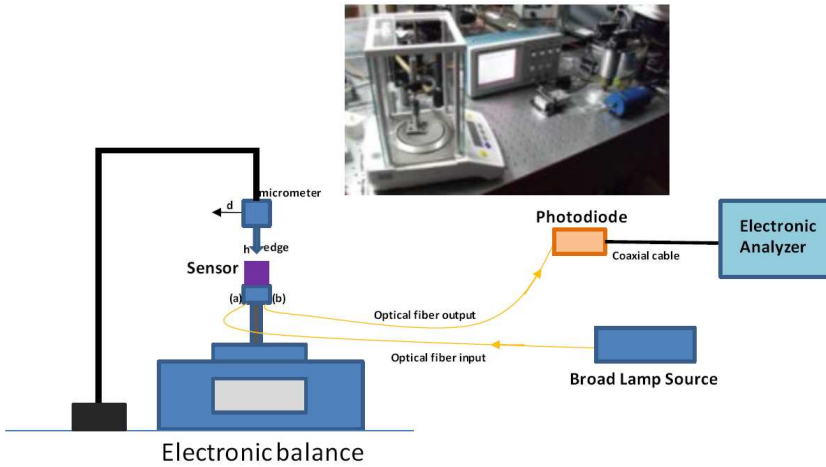


Figure 7. Scheme of the experimental setup concerning electric measurements. Inset: photo of the used experimental setup. The metallic edge has a resolution of 0.2 mm.

metallic edge which can be shifted by a micrometer in order to measure the sensor sensitivity in different surface regions of the sensor: the position h will define the applied pressure magnitudes (pressure along the vertical position), and the position d will shift the working point from the initial position. The input of the sensor is coupled with a broad lamp source. The output of sensor is connected with a Thorlabs DET 210 high speed silicon photo detector in order to convert the optical signal into an electric one. For its small dimensions this detector is suitable for an integration in a robotic arm. The pressure sensor sample is fixed on a system which assures the mechanical stability during the application of the pressure forces. The photodiode output is connected by means of a coaxial cable to a high sensitive electronic oscilloscope (TEKTRONIX TDS 220) which measures the electric signal corresponding to the variation of the optical intensity following the application of the pressure forces. The system of Fig. 7 allows to measure the variation ΔV of the voltage signal due to the application of the equivalent weights: in particular, as also observed from the optical measurements of Fig. 4 and Fig. 5, Fig. 8 shows that a reduction of transmitted signal ΔV corresponds to a well defined applied weights (the reference value $\Delta V = 0$ is the no-touching metallic edge case). As expected, we observe from Fig. 8 that the major pressure sensitivity is performed when the edge is exactly on the tapered region (maximum coupling efficiency corresponding to the position A): in this case an

Table 1. Overview of the measurements.

	Prototype of Fig. 1(a)	Prototype of Fig. 1(b)
Chemical composition	PDMS + gold precursor (concentration of 10% in weight)	PDMS + gold precursors (concentration of 10% in weight)
Order of Sensitivity	$\cong 5$ grams	$\cong 5$ grams
Elastomeric GNM time response at 0.098 N ($\cong 10$ grams)	$\cong 0.6$ sec.	$\cong 0.6$ sec.
Experimental setup	Sensor + micrometer mechanical stage + electronic balance + OMA	Sensor + electronic balance + micrometer mechanical stage + photodiode + numerical oscilloscope
Type of analysis	Optical signal processing (optical characterization); sensitivity versus λ	Electric signal processing (electric characterization); sensitivity versus different positions of the applied forces.
Possible range of applied weights	5 \div 50 grams	5 \div 150 grams

applied equivalent weight of 5 grams is enough to detect a variation of about $\Delta V = 2.5$ mV. The sensitivity of the sensor decreases by moving the edge in steps of 50 microns: a minimum variation of $\Delta V = 2.5$ mV is measured by applying a major equivalent weight of 13 grams for the position B (related to a shift $d = 50$ microns) and of 24 grams for the position C (related to a shift $d = 100$ microns), respectively. In order to highlight the differences between the optical characterization and the electric one of the two measured prototypes, we report in Table 1 the summary of the proposed measurements.

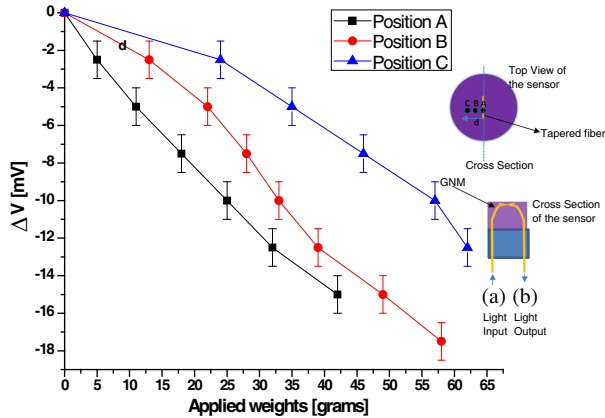


Figure 8. Electric measurements for different positions of the edge. Inset: top view and cross section of the measured pressure sensor.

5. CONCLUSIONS

In this work we presented a new concept of innovative optical tactile sensor based on PDMS-gold nanocomposite materials and its optical/electrical characterization. In particular, in this paper we propose a high sensitivity sensor which allows to measure pressure forces corresponding to weights of five grams and can be easily implemented in a tactile robotic systems including shape and dielectric permittivity sensing. The novel sensor is suitable for the implementation in a robotic hand system: its small dimension allows to consider the sensor as a robotic finger where the optical signal can be converted in an electrical one and, consecutively, processed in an intelligent robotic algorithm. The recognition can be addressed to the detection of shapes or surface roughness. The found aspects concerning the variation of the sensitivity with respect to exact position of the applied force can be used for signal processing tools for robotics. Other aspects such as the behavior of the sensor versus the temperature are under investigation.

REFERENCES

1. Firdaus, S. M., I. A. Azid, O. Sidek, K. Ibrahim, and M. Hussien, "Enhancing the resistivity of a mass-based piezoresistive micro-electro-mechanical systems cantilever sensor," *Micro & Nano Lett.*, Vol. 5, 85–90, 2010.

2. Kane, B. J., M. R. Cutkosaky, and T. A. Kovacs, "A traction stress sensor array for use in high resolution robotic tactile image," *J. Microelectromech. Syst.*, Vol. 9, 425–434, 2000.
3. Beebe, D. J., A. S. Hseih, D. D. Denton, and R. G. Radwin, "A silicon force sensor for robotics and medicine," *Sens. Actuator A*, Vol. 50, 55–56, 1995.
4. Lee, J. I., X. Huang, and P. B. Chu, "Nanoprecision MEMS capacitive sensor for linear and rotational positioning," *IEEE J. Microelectromech. Syst.*, Vol. 18, 660–670, 2009.
5. Gray, B. L. and R. S. Fearing, "A surface micromachined micro tactile sensor array," *Proceedings of the IEEE International Conference on Robotics and Automation*, 1–6, 1996.
6. Leineweber, M., G. Pelz, M. Schmoidt, H. Kappert, and G. Zimmer, "New tactile sensor chip with silicone rubber cover," *Sens. Actuator A*, Vol. 84, 236–245, 2000.
7. Li, C., P. M. Wu, L. A. Shutter, and R. K. Narayan, "Dual-mode operation of flexible piezoelectric polymer diaphragm for intracranial pressure measurement," *App. Lett.*, Vol. 96, 053502–053502-3, 2010.
8. Kolesar, E. S. and C. S. Dyson, "Object image with a piezoelectric robotic tactile sensor," *J. Microelectromech. Syst.*, Vol. 4, 87–96, 1995.
9. Reston, R. R. and E. S. Kolesar, "Robotic tactile sensor array fabricated from a piezoelectric polyvinylidene fluoride film," *Proceedings of the IEEE NAICON*, 1139–1144, 1990.
10. Heo, J. S., J. H. Chung, and J. J. Lee, "Tactile sensor array using fiber Bragg grating sensors," *Sens. Act. (A)*, Vol. 126, 312–327, 2006.
11. Massaro, A., F. Spano, P. Cazzato, R. Cingolani, and A. Athanassiou, "Real time optical pressure sensing for tactile detection using gold nanocomposite material," *Proceeding of MNE 2010*, 121–122, 2010.
12. Rakic, A., A. B. Djuricic, J. M. Elazar, and M. L. Majewski, "Optical properties of metallic films for vertical-cavity optoelectronic devices," *Appl. Opt.*, Vol. 37, 5271–5283, 1998.
13. Chen, M. and R. G. Horn, "Refractive index of sparse layers of absorbed gold nanoparticles," *Journ. of Coll. Interf. Science*, Vol. 315, 814–818, 2007.
14. Massaro, A., L. Pierantoni, and T. Rozzi, "Development of the EM coupling in laminated multilayered 3D optical waveguides," *Intern. J. Num. Model.*, Vol. 18, 237–253, 2005.

15. Massaro, A., V. Errico, T. Stomeo, A. Salhi, R. Cingolani, A. Passaseo, and M. De Vittorio, "3D FEM modeling and fabrication of circular photonic crystal microcavity," *IEEE J. Light. Technol.*, Vol. 26, 2960–2968, 2008.
16. Massaro, A., L. Pierantoni, and T. Rozzi, "Far-field radiation of optical fibers with tapered end," *IEEE J. Light. Technol.*, Vol. 24, 3162–3168, 2006.
17. Zhang, Q., J. J. Xu, Y. Liu, and H. Y. Cuen, "In-situ synthesis of poly(dimethylsiloxane)-gold nanoparticles composite films and its application in microfluidic system," *Lab on Chip*, Vol. 8, 352–357, 2008.
18. Hoppe, C. E., C. Ridriguez-Abreu, M. Lazzari, M. A. Lopez-Quintela, and C. Solans, "One-pot preparation of gold-elastomer nanocomposites using PDMS-graft-PEO copolymer micelles as nanoreactors," *Phys. Stat. Sol. (a)*, Vol. 205, 1455–1459, 2008.